

This **Supplemental Material** accompanies Batbaatar, J., Gillespie, A.R., Koppes, M., Clark, D.H., Chadwick, O.A., Fink, D., Matmon, A., and Rupper, S., 2020, Glacier development in continental climate regions of central Asia, in Waitt, R.B., Thackray, G.D., and Gillespie, A.R., eds., Untangling the Quaternary Period: A Legacy of Stephen C. Porter: Geological Society of America Special Paper 548, [https://doi.org/10.1130/2020.2548\(07\)](https://doi.org/10.1130/2020.2548(07)).

GSA Supplemental Material

for

Glacier development in continental climate regions of central Asia

Jigjidsurengiin Batbaatar^{1,*}, Alan R. Gillespie¹, Michele Koppes², Douglas H. Clark³,

Oliver A. Chadwick⁴, David Fink⁵, Ari Matmon⁶, Summer Rupper⁷

¹ *Quaternary Research Center, University of Washington, Seattle, WA 98195-1310, USA*

² *Department of Geography, University of British Columbia, Vancouver, BC V6T 1Z2, Canada*

³ *Department of Geology, Western Washington University, Bellingham, WA 98225-9160, USA*

⁴ *Department of Geography, University of California Santa Barbara, Santa Barbara, CA 93106, USA*

⁵ *Australian Nuclear Science and Technology Organisation, New Illawarra Rd, Lucas Heights NSW 2234, Australia*

⁶ *The Fredy and Nadine Herrmann Institute of Earth Sciences, The Hebrew University of Jerusalem,*

Edmond J. Safra Campus Givat Ram, Jerusalem 91904, Israel

⁷ *Department of Geography, University of Utah, Salt Lake City, UT 84112, USA*

* corresponding author email: bataa@uw.edu

List of Supplementary Tables provided in a spreadsheet (548-07-SuppMat-Tables.xlsx)

Table S1. ^{10}Be data

Table S2. ^{26}Al data

Table S3. Data for CRONUS-Earth online calculator version 2.3 (<http://hess.ess.washington.edu>)

Table S4. Outlier evaluation by normalized deviation method (Batbaatar et al., 2018)

Table S5. Outlier evaluation using Chauvenet's (Chauvenet, 1891) and Peirce's (Ross, 2003)
criteria

Table S6. Summary of outlier evaluations using Chauvenet's, Peirce's, and normalized deviation
criteria

Table S7. Mean ^{10}Be ages for groups with two samples

Table S8. Estimations of modern ELA

Table S9. Paleo ELA and ΔELA estimations

Table S10. Dated ΔELA and modern climate at the modern ELA

Selection of the study sites and literature data

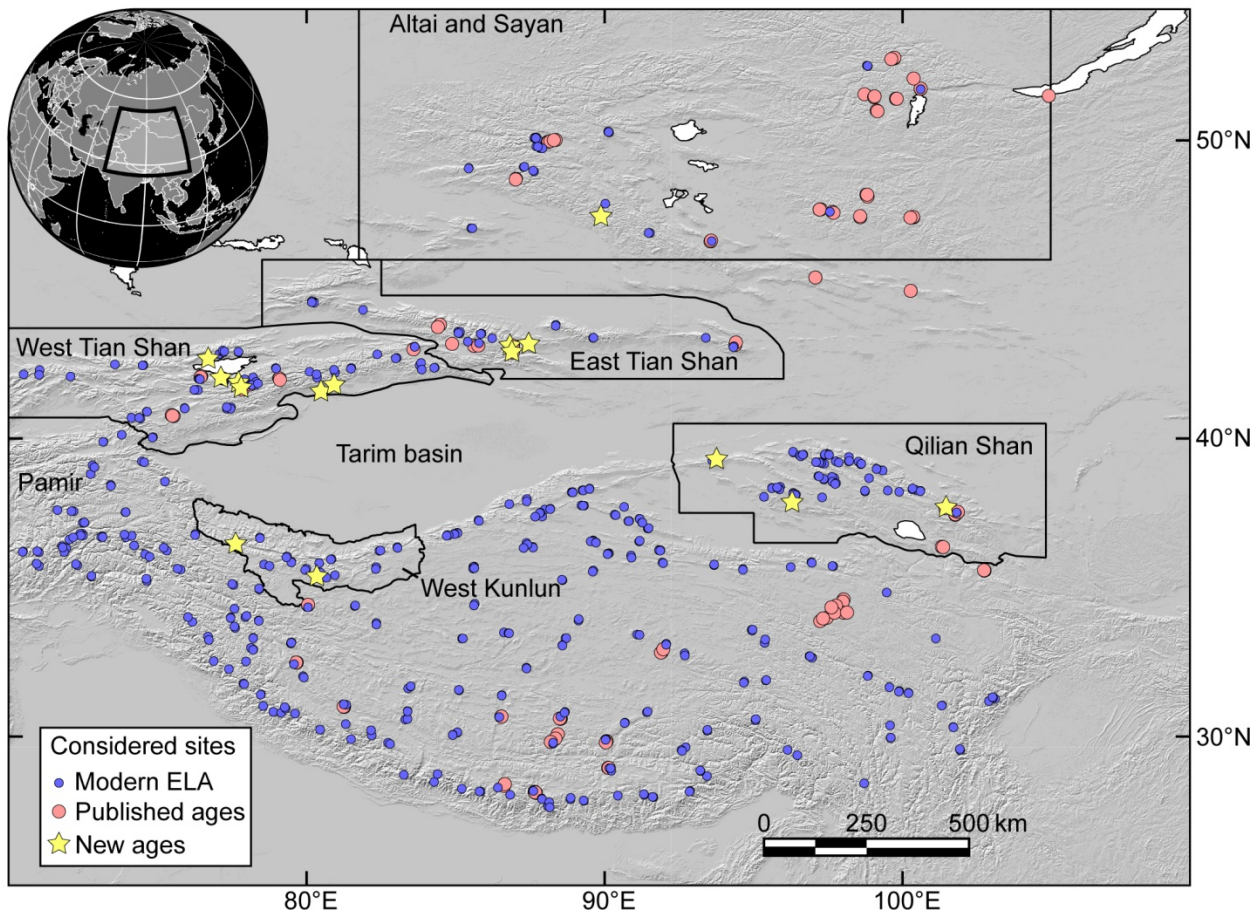


Figure S1. The sites considered in this study for modern and paleo ELAs. The locations of the modern glaciers are from Randolph Glacier Inventory 6.0 (RGI Consortium, 2017). The published ages are from the compilation by J. Heyman (<http://expage.github.io/data/expage/expage-201803.txt>, accessed 2018). The coordinates for all the sites and their respective references are provided in Supplementary Tables S4, S7, and S8.

Sensitivity of apparent exposure ages to boulder erosion

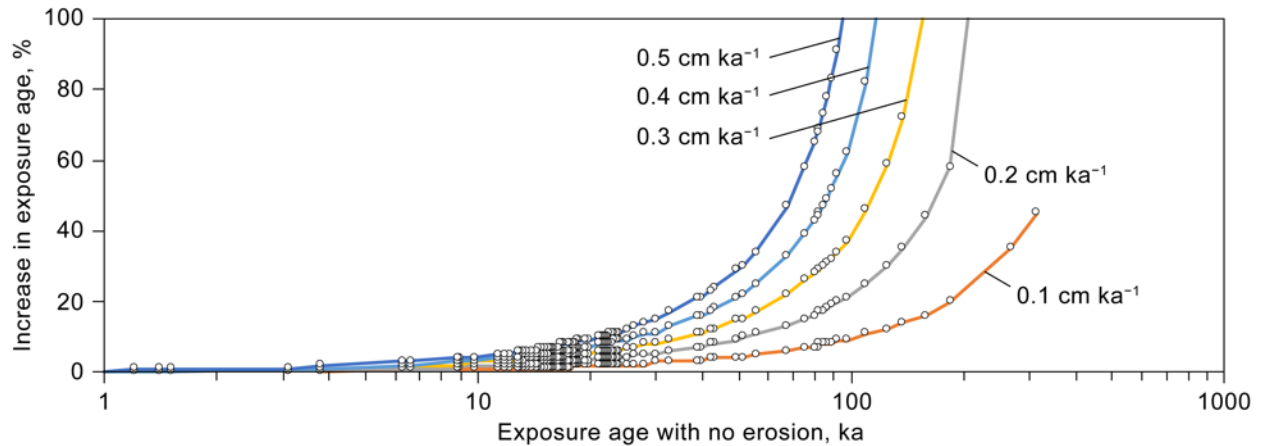


Figure S2. Increase in the apparent exposure ages if corrected for boulder erosion. All data points are for the new ages reported in this study. The increase in the exposure ages by more than 100% is excluded in the plot.

Quality assessment of the exposure ages

All researchers strive to acquire ages with high accuracy and high precision. Cosmic-ray exposure dating of moraines is not an exception, and many studies have developed a set of rules for this pursuit. Dortch et al. (2013) assumed that the ages from a moraine should be normally distributed and recommended accepting age groups with ≥ 3 ages and with the highest probability by visually evaluating the probability density function (PDF). In a similar approach, Owen and Dortch (2014) used Student's *t*-test to compare age groups for different sites. Another commonly used test to identify normally distributed ages is the reduced chi-squared statistic ($R\chi^2$; see Balco, 2011 and the references therein). For example, Heyman (2014), Hughes et al. (2016), and Small et al. (2017) required that a group should have ≥ 3 ages and exhibit a $R\chi^2$ value close to 1. After following the “robustness” classification system of Heyman (2014), Blomdin et al. (2016) and Gribenski et al. (2018) further required that the ratio of the mean age and 1σ total uncertainty (σ/μ) should be $\leq 15\%$.

Our approach in evaluating the ^{10}Be ages is similar to these statistical tests but differs in certain regards:

- 1) We used normalized deviation method of Batbaatar et al. (2018) to identify outliers in a group of ages. This method calculates a mean age excluding the tested age (excluded mean) and requires and identifies the tested age as outlier if the difference between the excluded mean and the tested ages was >2 than the compounded uncertainty of the excluded mean and the tested age.
- 2) We used Chauvenet's (1891) and Peirce's (Ross, 2003) criteria to check the outliers identified by normalized deviation method. In all instances, the normalized deviation method agreed with or identified more outliers than the other two criteria.
- 3) We accepted the age groups with two samples, including the groups that are left with two samples after rejecting the outlier(s).
- 4) We calculated $R\chi^2$ values for the age groups before and after rejecting the outliers with normalized deviation method. The $R\chi^2$ was not used as a criterion to reject outliers and was only provided for researchers to evaluate and render their own judgement.
- 5) We accepted the mean ages for groups with $\sigma/\mu < 50\%$. In doing so, we recognize that some ages with large uncertainty are accurate enough for the purpose of our broad comparison of glaciations between marine oxygen isotope stages at a scale of $>10^4$ yr, but not precise enough to make comparisons at $<10^4$ yr. For example, alpine glaciers respond to climate change in decades (Roe et al., 2017) and they can exhibit km-scale fluctuations around their end moraines in a steady climate without requiring a change in climate (Anderson et al., 2014). In other words, we recognize that some of the boulders on a moraine can be deposited at different times but within the limit of 2σ external uncertainty of ^{10}Be ages. Typical 1σ external uncertainty for ^{10}Be ages is $\sim 10\%$, and 2σ uncertainty would result in 4 ka uncertainty for a 20-ka sample).

Modern and MIS 2 ELA gradients along the latitude

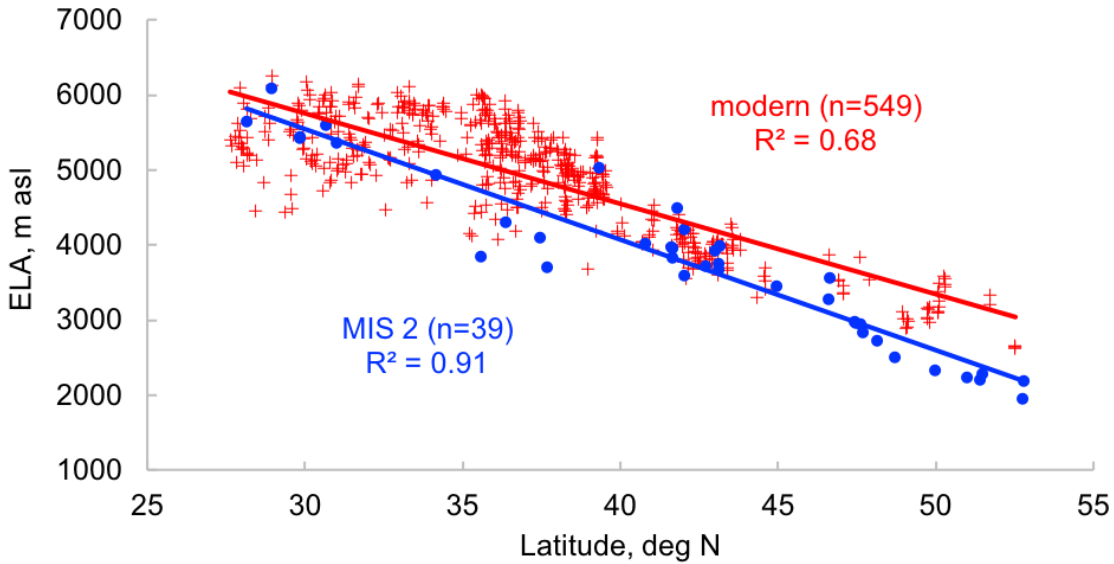


Figure S3. The modern ELAs (crosses) and the paleo-ELAs for the dated MIS 2 standstills (closed circles). This is the color version of Fig. 14A in the main text, in which the black and white data points are hard to distinguish. Modern and paleo-ELAs both show highly correlated latitudinal gradients, implying that the T_{air} and insolation are strong controls on glacier advances.

Photos of sampled boulders and surface features in the study sites



Figure S4. The sampled moraines near the Barskoon pass, Kyrgyzstan. The dashed lines indicate the moraine crests. Note the van in the foreground for scale. The photographer was facing southwest.



Figure S5. Boulder sample BS-001A (41.88323°N and 77.70568°E), on the crest of a moraine near Barskoon pass, Kyrgyzstan. The sledgehammer on the boulder is ~30 cm long.



Figure S6. Boulder sample BS-002 (41.88323°N and 77.70568°E), on a moraine near Barskoon pass, Kyrgyzstan. The sledgehammer on the boulder is ~ 30 cm long.



Figure S7. Boulder sample BS-004A (41.88288°N and 77.7061°E), on the crest of a moraine near Barskoon pass, Kyrgyzstan. Note the person walking on the crest of the sampled moraine. The photographer was facing south.



Figure S8. Boulder sample BS-007A (41.87017 °N and 77.73407 °E), on a moraine near Barskoon pass, Kyrgyzstan. Note the moraine crest that stretches from the boulder to the top of the photo. The glacier flowed from northwest to southeast (from top to bottom in the photo). The photographer was facing northwest.



Figure S9. View to the south from the location of boulder sample BS-007C (41.86975°N and 77.73563°E). The hummocky terrain, with telephone poles in the background, was the bed of a large glacier that flowed from west to east (from right to left in the photo). The photographer was facing southeast.



Figure S10. View to the south near the sampled moraine (42.01147°N and 77.1996°E), Gulbel pass, Kyrgyzstan. The people in the photo are walking on the slope of the right-lateral moraine of a paleoglacier that flowed southeast to northwest (from top left to bottom right in the photo). The photographer's approximate location was at 42.0219°N and 77.1836°E .



Figure S11. Panoramic view to the south from the location of the boulder sample GP-003A ($42.038133^{\circ}\text{N}$ and $77.142083^{\circ}\text{E}$), near Gulbel pass, Kyrgyzstan. Note the bouldery floor of the valley and the right-lateral moraines below the clouds (top left).



Figure S12. Panoramic view to the north of the hummocky valley floor, Choktal, Kyrgyzstan. The photo was taken at the location of boulder samples CR-001A–C (42.70139°N and 76.70089°E). Note the white shack in the middle for scale. The boulders on the crest of the left-lateral moraine (right) were sampled. A paleoglacier in this valley flowed from right to left.



Figure S13. Panoramic view to the northeast from the location of the boulder sample CR-003D (42.74707°N and 76.69433°E), Choktal, Kyrgyzstan. Due to optical distortion of the panoramic view the moraine crest in the foreground appears circular. The boulder samples CR-002A–E were taken from the moraine above the violet flower field in the middle of the photo.



Figure S14. Southward view of the Altyn Tagh range. The sampled moraine is from the glacier seen in the middle of the frame. The dust settling in the foreground emanates from the mining.



Figure S15. View to the southeast from the valley floor at Altyn Tagh. Note the people walking on the crest of a left-lateral moraine where boulder sample CAT-02C (39.3145°N and 93.74186°E) was taken. The dust from the mining down valley rose over the glacier by afternoon. Photo by Ari Matmon.



Figure S16. Boulder sample CAT-02C from Altyn Tagh. The cloth bag is ~30 cm wide.



Figure S17. The tongue of the glacier in the next valley (39.3213°N and 93.7230°E) to the west of the sampled moraine (Fig. S14). In this valley, an ice-cored moraine sits below the glacier and the hummocky surface in the foreground lies ~300 m from the glacier tongue. No other moraine was found in the valley.



Figure S18. Surface of the moraine sampled in Dumda valley, near Dunde ice cap (visible in the background). Note the low relief of the moraine surface and the rounded and embedded boulders. The photographer was facing northeast.



Figure S19. Boulder sample CH-DU-01 (37.85994°N and 96.28808°E), from Dumda valley, Dunde ice cap. Note the remnants of eroded boulders in the surrounding. The view of the photo is southward.



Figure S20. Boulder sample QS-GG-001 (37.69356 °N and 101.45208 °E) from Gangshiqia, Qilian Shan.



Figure S21. Boulder sample QS-GG-002 (37.69356 °N and 101.45208 °E) from Gangshiqia, Qilian Shan.



Figure S22. Boulder sample QS-GG-003 (37.69417 °N and 101.45319 °E) from Gangshiqia, Qilian Shan.



Figure S23. Boulder sample QS-GG-004 (37.69417 °N and 101.45319 °E) from Gangshiqia, Qilian Shan.



Figure S24. Boulder sample QS-GG-006 (37.69444°N and $101.45417^{\circ}\text{E}$) from Gangshiqia, Qilian Shan.



Figure S25. Boulder sample QS-GG-013 (37.65825°N and $101.43286^{\circ}\text{E}$) from Gangshiqia, Qilian Shan. The notebook on the boulder is ~20 cm long.



Figure S26. Terminus of the Quanshui glacier in 1995 (35.3996°N and 80.3720°E , 5460 m asl), Aksaiqin site, Kunlun. The proglacial lake is \sim 800 m across. The summer $T_{air} = -0.5 \pm 1.1^{\circ}\text{C}$; annual $ppt \sim 120$ mm. Photograph looking north, by Douglas H. Clark, 1995.



Figure S27. The view towards the terminus of the Quanshui glacier from the distal edge of the sampled end moraine (35.3982°N and 80.3710°E , 5460 m asl). The isolated proglacial lake in the left is about 200 m across. Photograph looking north, by Douglas H. Clark, 1995.



Figure S28. Heavily weathered granitic erratic on till plain ~300 m distal to the outer margin of the sampled moraine (36.4375°N and 77.6556°E , 5150 m asl), Karakax, Kunlun (Fig. 13B in main text). The sampled left lateral terminal moraine and the modern glacier are visible behind the erratic. The notepad in front of the erratic is ~30 cm long. White color on the ground around the boulders are surficial deposits of gypsum. The existence of gypsum and other soluble salt crystals and the lack of CaCO_3 in the soils provide evidence for hyperaridity in the region extending back for tens of thousands of years, suggesting that the glaciers there operated under low precipitation. Photograph looking north, by Douglas H. Clark, 1995.



Figure S29. Heavily weathered granitic erratic on till plain ~300 m distal to the outer margin of the sampled moraine (36.4375°N and 77.6556°E , 5150 m asl), Karakax, Kunlun (Fig. 13B in main text). The notepad in front of the erratic is ~30 cm long. White color on the ground around the boulders are surficial deposits of gypsum. The ELAs for the cirque glaciers visible in the background are ~5560 m asl. Photograph looking south, by Douglas H. Clark, 1995.



Figure S30. Left-lateral offset, ~3 m, of a modern channel along the active trace of the Altyn Tagh fault (36.4204°N and 77.6571°E , 4950 m asl), Karakax, Kunlun. Black backpack (~30 cm wide) just below the fault scarp (center) gives scale. Photograph looking north, by Douglas H. Clark, 1995.



Figure S31. Glaciated peaks and Glacier Station #2 viewed from the youngest moraine in Daxigou, Tian Shan. Photograph looking north, by Alan R. Gillespie, 1992.



Figure S32. Glaciated peaks viewed from the moraines sampled at Daxigou, Tian Shan.

Photograph looking east, by Alan R. Gillespie, 1992.



Figure S33. Modern glaciers in Daxigou, Tian Shan. The glacier on top is monitored from the Glacier Station #2. The two glaciers were in contact in 1992 and have retreated and separated since then. Photograph looking west, by Alan R. Gillespie, 1992.



Figure S34. The main trunk valley in Daxigou, Tian Shan. Glacier station #2 is visible in the foreground. Photograph looking east, by Alan R. Gillespie, 1992.



Figure S35. Overview of the two headwater glaciers in Daxigou, Tian Shan. Photograph looking west, by Alan R. Gillespie, 1992.



Figure S36. Surface features of the dated moraines in Tailan, Tian Shan. Photograph looking south towards the Taklamakan, by Alan R. Gillespie, 1992.

References Cited in the Supplemental Material

- Adler, R.F., Huffman, G.J., Chang, A., Ferraro, R., Xie, P., Janowiak, J., Rudolf, B., Schneider, U., Curtis, S., Bolvin, D., Gruber, A., Susskind, J., Arkin, P., 2003, The Version 2 Global Precipitation Climatology Project (GPCP) Monthly Precipitation Analysis (1979–Present): *Journal of Hydrometeorology*, v. 4, p. 1147–1167, [https://doi.org/10.1175/1525-7541\(2003\)004%3C1147:TVGCP%3E2.0.CO;2](https://doi.org/10.1175/1525-7541(2003)004%3C1147:TVGCP%3E2.0.CO;2).
- Amidon, W.H., Bookhagen, B., Avouac, J-P., Smith, T., Rood, D., 2013, Late Pleistocene glacial advances in the western Tibet interior: *Earth and Planetary Science Letters*, v. 381, p. 210–221, <https://doi.org/10.1016/j.epsl.2013.08.041>.
- Anderson, L.A., Roe, G.H., Anderson, R.S., 2014, The effects of interannual climate variability on the moraine record: *Geology*, v. 42, p. 55–58, <https://doi.org/10.1130/G34791.1>.
- Arzhannikov, S.G., Braucher, R., Jolivet, M., Arzhannikova, A.V., Vassallo, R., Chauvet, A., Bourlès, D., Chauvet, F., 2012, History of late Pleistocene glaciations in the central Sayan-Tuva Upland (southern Siberia): *Quaternary Science Reviews*, v. 49, p. 16–32, <https://doi.org/10.1016/j.quascirev.2012.06.005>.
- Balco, G., Stone, J.O., Lifton, N.A., Dunai, T.J., 2008, A complete and easily accessible means of calculating surface exposure ages or erosion rates from ^{10}Be and ^{26}Al measurements: *Quaternary Geochronology*, v. 3, p. 174–195, <https://doi.org/10.1016/j.quageo.2007.12.001>.
- Balco, G., 2011, Contributions and unrealized potential contributions of cosmogenic- nuclide exposure dating to glacier chronology, 1990–2010: *Quaternary Science Reviews*, v. 30, p. 3–27, <https://doi.org/10.1016/j.quascirev.2010.11.003>.
- Batbaatar, J., and Gillespie, A., 2016, Outburst floods of the Maly Yenisei. Part II – new age constraints from Darhad basin: *International Geology Review*, v. 58 (14), p. 1753–1779, <http://dx.doi.org/10.1080/00206814.2016.1193452>.
- Batbaatar, J., Gillespie, A., Fink, D., Matmon, A., Fujioka, T., 2018, Asynchronous glaciations in arid continental climate: *Quaternary Science Reviews*, v. 182, p. 1–19, <https://doi.org/10.1016/j.quascirev.2017.12.001>.
- Blomdin, R., Stroeven, A.P., Harbor, J.M., Lifton, N.A., Heyman, J., Gribenski, N., Petrakov, D.A., Caffee, M.W., Ivanov, M.N., Hättestrand, C., Rogozhina, I., 2016, Evaluating the timing of former glacier expansions in the Tian Shan: a key step towards robust spatial correlations: *Quaternary Science Reviews*, v. 153, p. 78–96, <https://doi.org/10.1016/j.quascirev.2016.07.029>.
- Chauvenet, W., 1891, A manual of spherical and practical astronomy, Vol II: Theory and use of astronomical instruments. Method of least squares, fifth edition, rev. and corr.: Philadelphia, J. B. Lippincott Co., p. 558–566.
- Chen, Y.X., Li, Y.K., Wang, Y.Y., Zhang, M., Cui, Z.J., Yi, C.L., 2015, Late Quaternary glacial history of the Karlik Range, easternmost Tian Shan, derived from ^{10}Be surface exposure and optically stimulated luminescence datings: *Quaternary Science Reviews*, v. 115, p. 17–27, <https://doi.org/10.1016/j.quascirev.2015.02.010>.

- Chevalier, M.L., Hillel, G., Tapponnier, P., Van der Woerd, J., Jing, L.Z., Finkel, R.C., Ryerson, F.J., Li, H.B., Liu, X.H., 2011, Constraints on the late Quaternary glaciations in Tibet from cosmogenic exposure ages of moraine surfaces: *Quaternary Science Reviews*, v. 30, p. 528–554, <https://doi.org/10.1016/j.quascirev.2010.11.005>.
- Colgan, P.M., Munroe, J.S., Zhou, S.Z., 2006, Cosmogenic radionuclide evidence for the limited extent of last glacial maximum glaciers in the Tanggula Shan of the central Tibetan Plateau: *Quaternary Research*, v. 65, p. 336–339, <https://doi.org/10.1016/j.yqres.2005.08.026>.
- Dong, G.C., Xu, X.K., Zhou, W.J., Fu, Y.C., Zhang, L., Li, M., 2017a, Cosmogenic ^{10}Be surface exposure dating and glacier reconstruction for the Last Glacial Maximum in the Quemuqu Valley, western Nyainqntanglha Mountains, south Tibet: *Journal of Quaternary Science*, v. 32, p. 639–652, <https://doi.org/10.1002/jqs.2963>.
- Dong, G.C., Zhou, W.J., Yi, C.L., Zhang, L., Li, M., Fu, Y.C., Zhang, Q., 2017b, Cosmogenic ^{10}Be surface exposure dating of ‘Little Ice Age’ glacial events in the Mount Jaggang area, central Tibet: *The Holocene*, v. 27, 1516–1525, <https://doi.org/10.1177%2F0959683617693895>.
- Dortch, J.M., Owen, L.A., Caffee, M.W., 2013, Timing and climatic drivers for glaciation across semi-arid western HimalayanTibetan orogen: *Quaternary Science Reviews*, v. 78, p. 188–208, <https://doi.org/10.1016/j.quascirev.2013.07.025>.
- Fan, Y., and van den Dool, H., 2008, A global monthly land surface air temperature analysis for 1948–present: *Journal of Geophysical Research*, v. 113, D01103, <https://doi.org/10.1029/2007JD008470>.
- Gillespie, A.R., Burke, R.M., Komatsu, G., Bayasgalan, A., 2008, Late Pleistocene glaciers in Darhad Basin, northern Mongolia: *Quaternary Research*, v. 69, p. 169–187, <https://doi.org/10.1016/j.yqres.2008.01.001>.
- Gribenski, N., Jansson, K.N., Lukas, S., Stroeven, A.P., Harbor, J.M., Blomdin, R., Ivanov, M.N., Heyman, J., Petrakov, D.A., Rudoy R., Clifton, T., Lifton, N.A., Caffee, M.W., 2016, Complex patterns of glacier advances during the late glacial in the Chagan Uzun Valley, Russian Altai: *Quaternary Science Reviews*, v. 149, p. 288–305, <https://doi.org/10.1016/j.quascirev.2016.07.032>.
- Gribenski, N., Jansson, K.N., Preusser, F., Harbor, J.M., Stroeven, A.P., Trauerstein, M., Blomdin, R., Heyman, J., Caffee, M.W., Lifton, N.A., Zhang, W., 2018, Re-evaluation of MIS 3 glaciation using cosmogenic radionuclide and single grain luminescence ages, Kanas Valley, Chinese Altai: *Journal of Quaternary Science*, v. 33, p. 55–67, <https://doi.org/10.1002/jqs.2998>.
- Heyman, J., Stroeven, A.P., Caffee, M.W., Hätteström, C., Harbor, J.M., Li, Y.K., Alexanderson, H., Zhou, L.P., Hubbard, A., 2011, Palaeoglaciology of Bayan Har Shan, NE Tibetan Plateau: exposure ages reveal a missing LGM expansion: *Quaternary Science Reviews*, v. 30, p. 1988–2001, <https://doi.org/10.1016/j.quascirev.2011.05.002>.
- Heyman, J., 2014, Paleoglaciation of the Tibetan Plateau and surrounding mountains based on exposure ages and ELA depression estimates: *Quaternary Science Reviews*, v. 91, p. 30–41, <https://doi.org/10.1016/j.quascirev.2014.03.018>.

- Heyman, J., 2018, A global compilation of glacial ^{10}Be and ^{26}Al data, <http://expage.github.io/data/expage/expage-201803.txt> (accessed March 2018).Horiuchi, K., Matsuzaki, H., Osipov, E., Khlystov, O., Fujii, S., 2004, Cosmogenic ^{10}Be and ^{26}Al dating of erratic boulders in the southern coastal area of Lake Baikal, Siberia: Nuclear Instruments and Methods in Physics Research B, v. 223–224, p. 633–638, <https://doi.org/10.1016/j.nimb.2004.04.117>.
- Hubert-Ferrari, A., Suppe J., Van der Woerd J., Wang X., Lu HF., 2005, Irregular earthquake cycle along the southern Tianshan front, Aksu area, China: Journal of Geophysical Research, v. 110, B06402, <https://doi.org/10.1029/2003JB002603>.
- Hughes, A.L.C., Gyllencreutz, R., Lohne, Ø.S., Mangerud, J., Svendsen, J.I., 2016, The last Eurasian ice sheets – a chronological database and time-slice reconstruction, DATED-1: Boreas, v. 45, p. 1–45, <https://doi.org/10.1111/bor.12142>.
- Kalnay, E., Kanamitsu, M., Kistler, R., Collins, W., Deaven, D., Derber, J., Gandin, L., Saha, S., White, G., Woollen, J., Zhu, Y., Chelliah, M., Ebisuzaki, W., Higgins, W., Janowiak, J., Mo, K.C., Ropelewski, C., Wang, J., Leetma, A., Reynolds, R., Jenne, R., 1996, The NCEP/NCAR 40-year re-analysis project: Bulletin of American Meteorological Society, v. 77, p. 437–471, [https://doi.org/10.1175/1520-0477\(1996\)077%3C0437:TNYRP%3E2.0.CO;2](https://doi.org/10.1175/1520-0477(1996)077%3C0437:TNYRP%3E2.0.CO;2).
- Kong, P., Fink, D., Na, C.G., Huang, F.X., 2009, Late Quaternary glaciation of the Tianshan, Central Asia, using cosmogenic ^{10}Be surface exposure dating: Quaternary Research, v. 72, p. 229–233, <https://doi.org/10.1016/j.yqres.2009.06.002>.
- Koppes, M., Gillespie, A.R., Burke, R.M., Thompson, S.C., Stone, J., 2008, Late quaternary glaciation in the Kyrgyz Tien Shan: Quaternary Science Reviews, v. 27, p. 846–866, <https://doi.org/10.1016/j.quascirev.2008.01.009>.
- Lasserre, C., Gaudemer, Y., Tapponnier, P., Mériaux, A-S., Van der Woerd, J., Yuan, D.Y., Ryerson, F.J., Finkel, R.C., Caffee, M.W., 2002, Fast late Pleistocene slip rate on the Leng Long Ling segment of the Haiyuan fault, Qinghai, China: Journal of Geophysical Research, v. 107, No. B11 2276, <https://doi.org/10.1029/2000JB000060>.
- Li, Y.K., Liu, G.N., Chen, Y.X., Li, Y.N., Harbor, J., Stroeven, A.P., Caffee, M., Zhang, M., Li, C.C., Cui, Z.J., 2014, Timing and extent of Quaternary glaciations in the Tianger Range, eastern Tian Shan, China, investigated using ^{10}Be surface exposure dating: Quaternary Science Reviews, v. 98, p. 7–23, <https://doi.org/10.1016/j.quascirev.2014.05.009>.
- Li, Y.K., Liu, G.N., Kong, P., Harbor, J., Chen, Y.X., Caffee M., 2011, Cosmogenic nuclide constraints on glacial chronology in the source area of the Urumqi River, Tian Shan, China: Journal of Quaternary Science, v. 26, p. 297–304, <https://doi.org/10.1002/jqs.1454>.
- Li, Y.N., Li, Y.K., Harbor, J., Liu, G.N., Yi, C.L., Caffee, M.W., 2016, Cosmogenic ^{10}Be constraints on Little Ice Age glacial advances in the eastern Tian Shan, China: Quaternary Science Reviews, v. 138, p. 105–118, <https://doi.org/10.1016/j.quascirev.2016.02.023>.Lifton, N., Beel, C., Hättestrand, C., Kassab, C., Rogozhina, I., Heermance, R., Oskin, M., Burbank, D., Blomdin, R., Gribenski, N., Caffee, M., Goehring, B.M., Heyman, J., Ivanov, M., Li, Y.N., Li, Y.K., Petrakov, D., Usualiev, R., Codilean, A.T., Chen, Y.X., Harbor, J., Stroeven, A.P.,

- 2014, Constraints on the late Quaternary glacial history of the Inylchek and Sary-Dzaz valleys from *in situ* cosmogenic ^{10}Be and ^{26}Al , eastern Kyrgyz Tian Shan: Quaternary Science Reviews, v. 101, p. 77–90, <https://doi.org/10.1016/j.quascirev.2014.06.032>.
- Liu, J.H., Yi, C.L., Li, Y.K., Bi, W.L., Zhang, Q., Hu, G., 2017, Glacial fluctuations around the Karola Pass, eastern Lhagoi Kangri range, since the Last Glacial Maximum: Journal of Quaternary Science, v. 32, p. 516–527, <https://doi.org/10.1002/jqs.2946>.
- Owen, L.A., Ma, H.Z., Derbyshire, E., Spencer, J.Q., Barnard, P.L., Nian, Z.Y., Finkel, R.C., Caffee, M.W., 2003a, The timing and style of late Quaternary glaciation in the La Ji Mountains, NE Tibet: evidence for restricted glaciation during the latter part of the last glacial: Zeitschrift für Geomorphologie Supplement, v. 130, p. 263–276.
- Owen, L.A., Spencer, J.Q., Ma, H.Z., Barnard, P.L., Derbyshire, E., Finkel, R.C., Caffee, M.W., Nian, Z.Y., 2003b, Timing of Late Quaternary glaciation along the southwestern slopes of the Qilian Shan, Tibet. Boreas, v. 32, p. 281–291, <https://doi.org/10.1111/j.1502-3885.2003.tb01083.x>.
- Owen, L.A., Finkel, R.C., Barnard, P.L., Ma, H.Z., Asahi, K., Caffee, M.W., Derbyshire, E., 2005, Climatic and topographic controls on the style and timing of late Quaternary glaciation throughout Tibet and the Himalaya defined by ^{10}Be cosmogenic radionuclide surface exposure dating. Quaternary Science Reviews, v. 24, p. 1391–1411, <https://doi.org/10.1016/j.quascirev.2004.10.014>.
- Owen, L.A., Dortch, J.M., 2014, Nature and timing of Quaternary glaciation in the Himalayan–Tibetan orogen: Quaternary Science Reviews, v. 88, p. 14–54, <https://doi.org/10.1016/j.quascirev.2013.11.016>.
- Rades, E.F., Hetzel, R., Strobl, M., Xu, Q., Ding, L., 2015, Defining rates of landscape evolution in a south Tibetan graben with *in situ*-produced cosmogenic ^{10}Be : Earth Surface Processes and Landforms, v. 40, p. 1862–1876, <https://doi.org/10.1002/esp.3765>.
- Reuther, A.U., 2007, Surface exposure dating of glacial deposits from the last glacial cycle – evidence from the eastern Alps, the Bavarian Forest, the southern Carpathians and the Altai Mountains: Relief Boden Paläoklima, v. 21, 213 p.
- RGI Consortium, 2017, Randolph Glacier Inventory – A Dataset of Global Glacier Outlines: Version 6.0: Technical Report, Global Land Ice Measurements from Space, Colorado, USA, <https://doi.org/10.7265/N5-RGI-60> (accessed March 2018).
- Roe, G.H., Baker, M.B., Herla, F., 2017, Centennial glacier retreat as categorical evidence of regional climate change: Nature Geoscience, v. 10, p. 95–99, <https://doi.org/10.1038/ngeo2863>.
- Ross, S.M., 2003, Peirce's criterion for the elimination of suspect experimental data: Journal of Engineering Technology, v. 20, p. 38–41, <http://classes.engineering.wustl.edu/2009/fall/che473/handouts/OutlierRejection.pdf>.
- Rother, H., Lehmkuhl, F., Fink, D., Nottebaum, V., 2014, Surface exposure dating reveals MIS-3 glacial maximum in the Khangai Mountains of Mongolia: Quaternary Research, v. 82, p. 297–308, <https://doi.org/10.1016/j.yqres.2014.04.006>.

- Schäfer, J.M., Tschudi, S., Zhao, Z.Z., Wu, X.H., Ivy-Ochs, S., Wieler, R., Baur, H., Kubik, P.W., Schlüchter, C., 2002, The limited influence of glaciations in Tibet on global climate over the past 170 000 yr: *Earth and Planetary Science Letters*, v. 194, 287–297, [https://doi.org/10.1016/S0012-821X\(01\)00573-8](https://doi.org/10.1016/S0012-821X(01)00573-8).
- Small, D., Clark, C.D., Chiverrell, R.C., Smedley, R.K., Bateman, M.D., Duller, G.A.T., Ely, J.C., Fabel, D., Medialdea, A., Moreton, S.G., 2017, Devising quality assurance procedures for assessment of legacy geochronological data relating to deglaciation of the last British-Irish Ice Sheet: *Earth-Science Reviews*, v. 164, p. 232–250, <https://doi.org/10.1016/j.earscirev.2016.11.007>.
- Smith, S.G., Wegmann, K.W., Ancuta, L.D., Gosse, J.C., Hopkins, C.E., 2016, Paleotopography and erosion rates in the central Hangay Dome, Mongolia: landscape evolution since the mid-Miocene: *Journal of Asian Earth Sciences*, v. 125, p. 37–57, <https://doi.org/10.1016/j.jseaes.2016.05.013>.
- Wang, J., Kassab, C., Harbor, J.M., Caffee, M.W., Cui, H., Zhang, G.L., 2013, Cosmogenic nuclide constraints on late Quaternary glacial chronology on the Dalijia Shan, northeastern Tibetan Plateau: *Quaternary Research*, v. 79, p. 439–451, <https://doi.org/10.1016/j.yqres.2013.01.004>.
- Zech, R., 2012, A late Pleistocene glacial chronology from the Kitschi-Kurumdu Valley, Tien Shan (Kyrgyzstan), based on ^{10}Be surface exposure dating: *Quaternary Research*, v. 77, p. 281–288, <https://doi.org/10.1016/j.yqres.2011.11.008>.
- Zhang, M., Chen, Y.X., Li, Y.K., Liu, G.N., 2016, Late Quaternary glacial history of the Nalati Range, central Tian Shan, China, investigated using ^{10}Be surface exposure dating: *Journal of Quaternary Science*, v. 31, p. 659–670, <https://doi.org/10.1002/jqs.2891>.